
On the effect of Batch Normalization and Weight Normalization in Generative Adversarial Networks

Sitao Xiang

Department of Computer Science
University of Southern California
Los Angeles, CA 90089
sitaoxia@usc.edu

Hao Li

Department of Computer Science
University of Southern California
Los Angeles, CA 90089
hao@hao-li.com

Abstract

As in many neural network architectures, the use of Batch Normalization (BN) has become a common practice for Generative Adversarial Networks (GAN). In this paper, we propose using Euclidean reconstruction error on a test set for evaluating the quality of GANs. Under this measure, together with a careful visual analysis of generated samples, we found that while being able to speed training during early stages, BN may have negative effects on the quality of the trained model and the stability of the training process. Furthermore, Weight Normalization, a more recently proposed technique, is found to improve the reconstruction, training speed and especially the stability of GANs, and thus should be used in place of BN in GAN training.

1 Introduction

Despite being widely used in Generative Adversarial Networks (GAN), the effect of Batch Normalization (BN) in GANs has not been carefully examined. This is partly due to the lack of a good measure of the quality of GAN models. Without such a quality metric, the use of BN is usually justified by that it is perceived to accelerate and stabilize training [11].

Not convinced by the claimed benefits of BN, we proposed a method to evaluate the quality, mode coverage in particular, of GAN models: performing gradient descent on the latent code to try to generate given samples from a test set not contained in the training samples and taking the mean Euclidean distance between the test samples and closest generated samples.

We found that the reconstruction error correlates well with the visual quality of the generated samples, and while still time consuming, it is much more affordable than existing evaluation methods such as log-likelihood estimation, and thus can be used to monitor the progress during training.

We show that BN does help with the training of GANs in that on some datasets and with some network structure, the use of BN makes training possible while otherwise training fails constantly, and that BN speeds up training in its early stage. On the other hand, when training is possible without BN, models trained with BN may actually be less stable and worse at generalizing.

Parallel to BN, we examined a more recently proposed technique called Weight Normalization (WN) [12] with the same set of experiments, and found that it does actually achieve the claimed benefits of BN in that it accelerates and stabilizes training, and gives models with equal or better quality than models without normalization. Thus, we propose WN as a superior alternative to BN in the context of GANs.

2 Related work

Batch Normalization Batch Normalization (BN) [8] is a technique to accelerate training of deep networks. It has been proved effective in many applications and has become a standard building block of modern neural network architectures. In GANs, It has been used in the influential DCGAN architecture [11] and has since become a common practice, as listed in this comprehensive list of GAN tricks [4].

To put it short, BN takes a batch of samples $\{x_1, x_2, \dots, x_m\}$ and does the following computation:

$$y_i = \frac{x_i - \mu_{\mathcal{B}}}{\sigma_{\mathcal{B}}} \cdot \gamma + \beta$$

where $\mu_{\mathcal{B}}$ and $\sigma_{\mathcal{B}}$ are the mean and standard deviation of the input batch and γ and β are learned parameters. The effect is that the output will always have mean β and standard deviation γ , regardless of the input distribution. Critically, the gradients must be back-propagated through the computation of $\mu_{\mathcal{B}}$ and $\sigma_{\mathcal{B}}$.

Weight Normalization Weight Normalization (WN) [12] is another relatively new such technique that is yet to see wide use. In a linear layer of the form

$$\mathbf{y} = \mathbf{W}^T \mathbf{x} + \mathbf{b} \tag{1}$$

where $\mathbf{x} \in \mathbb{R}^n$, $\mathbf{y} \in \mathbb{R}^m$, $\mathbf{W} \in \mathbb{R}^{n \times m}$ and $\mathbf{b} \in \mathbb{R}^m$, weight normalization reparametrizes \mathbf{W} as $\mathbf{V} \in \mathbb{R}^{n \times m}$ and $\mathbf{g} \in \mathbb{R}^m$:

$$\mathbf{w}_i = \frac{g_i}{\|\mathbf{v}_i\|} \cdot \mathbf{v}_i \tag{2}$$

where \mathbf{w}_i and \mathbf{v}_i are the i -th column of \mathbf{W} and \mathbf{V} , respectively. Similar to BN, computation of $\|\mathbf{v}_i\|$ is taken into account when computing the gradient with respect to \mathbf{V} .

Although presented as a reparametrization that modifies the curvature of the loss function, we consider the idea of dividing the weight vector by its norm intuitive and straightforward. Indeed, a very similar idea has been proposed at around the same time under the name “normalization propagation” (NormProp) [2].

The effectiveness of this technique has been illustrated by various experiments in [12] and [2]. They did not include any experiment with GAN, which is what we will do here.

The detail of our version of Weight Normalization is slightly different to both [12] and [2], which will be explained in section 3.

Evaluation of GANs The most widely used (e.g. in [5][6]) method to evaluate GANs has been visually inspecting the quality of generated samples, e.g. by finding the closest training sample to generated samples and pointing out their difference or interpolating between codes, and estimating the log-likelihood of a separate set of test samples by fitting a Gaussian Parzen window. As discussed in [13], these are generally ineffective as subtle overfitting could be hard to visually detect and to get even close to the true log-likelihood would require an unrealistically large number of samples.

GANs have also been evaluated indirectly, e.g. by testing classification accuracy with features extracted by the GAN discriminator [11].

Beside the quality of GANs, various alternative form of training loss has been proposed to monitor the training process [1] [3].

3 Alternative version of weight normalization

A notable deficiency of WN is that, in its simplest form, it does not try to normalize the mean of the input. In [12] this is solved by augmenting WN with a version of BN that only normalizes the mean of the input but not the variance. While their experiments showed a improved performance in CIFAR-10 classification task comparing to plain WN, in our experiments it gave worse results, so we chose to not include this augmentation. (See appendix C.2 for experiments)

In [2], the authors attempted to solve this by enforcing a zero-mean, unit-variance distribution throughout the network. Their proposed method is to first use a restricted form of Weight Normalization,

where the scale factor $\mathbf{g} = \mathbf{1}$ and bias $\mathbf{b} = \mathbf{0}$, that is (for simplicity of notation we consider a single output neuron in this section),

$$y = \frac{\mathbf{w}^T \mathbf{x}}{\|\mathbf{w}\|} \quad (3)$$

and normalize the training data so that the input to the network have zero mean and unit variance, then evaluate the mean and variance of the output of each nonlinear layer (ReLU in their example) in closed form under the assumption that the input to the preceding linear layer is from a multivariate standard normal distribution. The mean and variance is then used to correct the distribution of the output:

$$y = \frac{1}{\sigma} \left[\text{ReLU} \left(\frac{\mathbf{w}^T \mathbf{x}}{\|\mathbf{w}\|} \right) - \mu \right] \quad (4)$$

where

$$\mu = \sqrt{\frac{1}{2\pi}} \quad \text{and} \quad \sigma = \sqrt{\frac{1}{2} \left(1 - \frac{1}{\pi} \right)}$$

are the mean and standard deviation of the distribution after ReLU when \mathbf{x} is from a multivariate standard normal distribution. The output y in equation 4 would also have zero mean and unit variance.

We wish to point out that this attempted fix does not achieve its goal. Firstly, as the authors themselves have mentioned, the closed form mean and variance is merely an approximation since the condition required for the correctness of the derivation does not hold beyond the first layer. But more importantly, after equation 4 is derived, the authors argued that as in BN, so as to not reduce the set of functions that can be represented by the network, they needed to introduce a learned affine transformation after the weight-normalized linear layer and before the succeeding non-linear layer. Thus the formula would become

$$y = \frac{1}{\sigma} \left[\text{ReLU} \left(\frac{\gamma (\mathbf{w}^T \mathbf{x})}{\|\mathbf{w}\|} + \beta \right) - \mu \right] \quad (5)$$

Their derivation for μ and σ is for the restricted case where there is no learned affine transformation, i.e. when $\gamma = 1$ and $\beta = 0$. When this restriction is relaxed, the result would be invalid even if the condition on \mathbf{x} does hold. We can, of course, make μ and σ functions of γ and β to fix this error. But this makes the computation over-complex as now to compute the gradient with respect to the parameters, these functions also need to be taken into account. And it is not worthwhile considering that such a complex formula is still merely an approximation when the condition on \mathbf{x} does not hold.

Since we cannot hope to strictly enforce a zero-mean unit-variance distribution, we use a cheap approximation instead. Note that with ReLU-like nonlinearity (i.e. ReLU, leaky ReLU and parametric ReLU) we have $\text{ReLU}(ax) = a \cdot \text{ReLU}(x)$ when $a \geq 0$. In equation 5, when $\gamma < 0$, we can always invert the direction of \mathbf{w} and take the negative of γ , so without loss of generality we can assume $\gamma \geq 0$. Then equivalently, equation 5 can be written as

$$y = \frac{\gamma}{\sigma} \left[\text{ReLU} \left(\frac{\mathbf{w}^T \mathbf{x}}{\|\mathbf{w}\|} + \frac{\beta}{\gamma} \right) - \frac{\mu}{\gamma} \right] \quad (6)$$

The purpose of μ and σ is to cancel the non-zero mean and non-unit variance introduced by ReLU, i.e. β and γ . Instead of deriving complex formulas, we elect to just take $\mu = \beta$ and $\sigma = \gamma$ and rewrite the formula with $\alpha = -\frac{\beta}{\gamma} = -\frac{\mu}{\gamma}$. Then, equation 6 becomes

$$y = \text{ReLU} \left(\frac{\mathbf{w}^T \mathbf{x}}{\|\mathbf{w}\|} - \alpha \right) + \alpha \quad (7)$$

Note that we can now separate the restricted weight normalized layer out from equation 7. We call the remaining part “Translated ReLU (TReLU)”:

$$\begin{aligned} \text{TReLU}_\alpha(x) &= \text{ReLU}(x - \alpha) + \alpha \\ &= \begin{cases} x & (x \geq \alpha) \\ \alpha & (x < \alpha) \end{cases} \end{aligned}$$

where α is a learned parameter. It translates the data, applies the nonlinearity, then translates the data back. Using TReLU instead of adding bias to the previous layer has the benefit of preventing (to a certain degree) the introduction of a large mean to the distribution while not damaging the expressiveness of the network. With other ReLU-like nonlinearity we can also have translated leaky and parametric ReLU.

Such a simplification does reduce the set of functions that can be represented by the network. But allowing an affine transformation to be learned at the last weight-normalized layer recovers the expressiveness of a full stack of layers (see appendix A for proof). From here on, “strict weight-normalized layers” would be used to refer to layers without affine transformation (equation 3), while layers with a learned affine transformation

$$y = \frac{\mathbf{w}^T \mathbf{x}}{\|\mathbf{w}\|} \cdot \gamma + \beta$$

would be referred to as “affine weight-normalized layers”. They are collectively called “weight-normalized layers”

4 Evaluation method

Some form of reconstruction error is often (part of) the objective to be optimized in generative models, e.g. in Variational Autoencoders [9]. Thus it is natural to evaluate generative models by reconstruction error on a test set. In the case of GANs, for a generator G and a set of test samples $X = \{x^{(1)}, x^{(2)}, \dots, x^{(m)}\}$, the reconstruction loss of G on X is defined as

$$\mathcal{L}_{\text{rec}}(G, X) = \frac{1}{m} \sum_{i=1}^m \min_z \|G(z) - x^{(i)}\|^2$$

Since there is no way to directly infer the optimal z from x , we use an alternative method: starting from an all-zero vector, we perform gradient descent on the latent code to find one that minimizes the Euclidean distance between the sample generated from the code and the target sample.

Since the code is optimized instead of computed from a feedforward network, the evaluation process is time-consuming. Thus, we perform this evaluation only infrequently during training to monitor the process and use a reduced number of samples and gradient descent steps. When evaluating the final trained model, we perform the evaluation on a larger test set with a larger number of steps.

Intuitively, in order to be able to generate the test samples that are not in the training set, the generator must learn the distribution of the training samples but not memorize and overfit on them. Thus reconstruction loss is a quantitative alternative to just visually inspecting the samples to detect overfitting and measuring the ability to generate novel yet plausible samples.

5 Experiments

5.1 Setup

We conducted the experiments on image generation task on central 160×160 patches of the CelebA dataset [10], with DCGAN [11] based models. We compared three models: model without any form of normalization as a reference (the non-normalized or “vanilla” model), model with Batch

Table 1: Network structure for discriminators (left) and generators (right). First three columns: type of layers for vanilla, BN and WN models, respectively. Forth column: kernel size, stride, padding and number of output channels of convolution layer.

vanilla	BN	WN		vanilla	BN	WN	
Conv	Conv	SWNConv	4, 2, 1, 64	Deconv	Deconv	SWNDeconv	5, 1, 0, 1024
-	-	-		-	BN	-	
PReLU	PReLU	TPReLU		PReLU	PReLU	TPReLU	
Conv	Conv	SWNConv	4, 2, 1, 128	Deconv	Deconv	SWNDeconv	4, 2, 1, 512
-	BN	-		-	BN	-	
PReLU	PReLU	TPReLU		PReLU	PReLU	TPReLU	
Conv	Conv	SWNConv	4, 2, 1, 256	Deconv	Deconv	SWNDeconv	4, 2, 1, 256
-	BN	-		-	BN	-	
PReLU	PReLU	TPReLU		PReLU	PReLU	TPReLU	
Conv	Conv	SWNConv	4, 2, 1, 512	Deconv	Deconv	SWNDeconv	4, 2, 1, 128
-	BN	-		-	BN	-	
PReLU	PReLU	TPReLU		PReLU	PReLU	TPReLU	
Conv	Conv	SWNConv	4, 2, 1, 1024	Deconv	Deconv	SWNDeconv	4, 2, 1, 64
-	BN	-		-	BN	-	
PReLU	PReLU	TPReLU		PReLU	PReLU	TPReLU	
Conv	Conv	AWNConv	5, 1, 0, 1	Deconv	Deconv	AWNDeconv	4, 2, 1, 3
Sigmoid	Sigmoid	Sigmoid		Sigmoid	Sigmoid	Sigmoid	

Normalization (“BN model”), and model with our formulation of Weight Normalization (“WN model”). The network is constructed in the following way: for discriminator, we use successive convolution layers with kernel size 4, stride 2, padding 1 and output channels doubling the previous layer, starting from 64, until the spatial size of the feature map is sufficiently small (5×5 in this case), then add one final convolution layer with stride 1, no padding and kernel size equal to the last feature map. For generator, these layers are exactly reversed.

As per common practice, Batch Normalization is not applied to the first layer of discriminator and last layer of both discriminator and generator. Weight normalization is applied to every layer. For the last layer of both discriminator and generator, we use affine weight-normalized layers (AWNConv and AWNDeconv in the table) while for every other layer we use strict weight-normalized layers (SWNConv and SWNDeconv). We use Parametric ReLU (PReLU) for vanilla and batch-normalized models and Translated Parametric ReLU (TPReLU) for weight-normalized models. Slope and bias parameters are learned per-channel. The length of the code is 256 for all models. Architectures are summarized in table 1.

We also found that weight initialization (more specifically, of the first layer of generator) had an impact on the effectiveness of WN. In our experiments, the weights of the weight-normalized layers are initialized with random numbers drawn uniformly from $[-t/\sqrt{c_I \cdot w_K \cdot h_K}, t/\sqrt{c_I \cdot w_K \cdot h_K}]$ where c_I , w_K and h_K are number of input channels, kernel width and kernel height respectively, and t is a scale factor. We set $t = 0.01$ for first layer of generator and $t = 1$ for every other layer. An $\varepsilon = 10^{-6}$ is added when computing the norm of weight vectors for numerical stability.

All models are optimized with RMSProp [14], with a learning rate of 10^{-4} and a batch size of 32. Specifically for the BN model, when training the discriminator, we use separate batches for true samples and generated samples, as suggested by [4].

After each parameter update, we clip the learned slope of parametric ReLU layers to $[0, 1]$.

There are a total of 202,599 images in CelebA dataset. We randomly selected 2,000 images for evaluation and used the rest for training. During the training, we perform the evaluation every 500 training iterations, on a randomly selected and fixed subset of 200 test samples. The optimal code is found by performing gradient descent for 50 steps, starting from a zero vector. Again we use RMSProp, with a learning rate of 0.01.

For each model, the best performing network during the training procedure is saved and used for final evaluation. In the final evaluation, we use all 2,000 test samples and perform gradient descent for 2,000 steps. For BN model, we use its inference mode.

Due to a phenomenon in which a model with worse 50-step reconstruction may give better 2,000-step reconstruction (as occurred in additional experiments in appendix C), we also take the “final” model

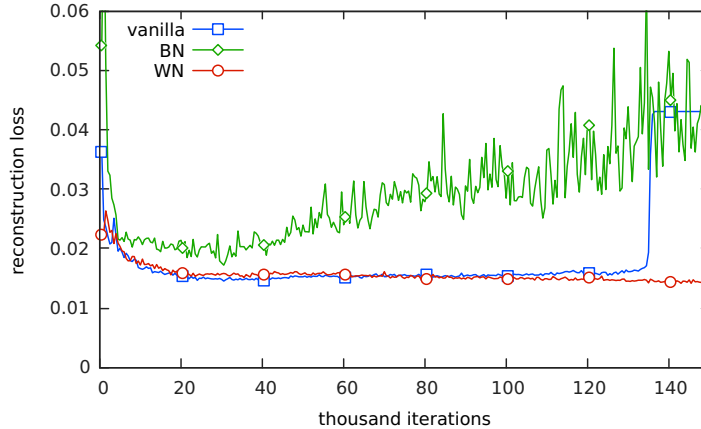


Figure 1: 50-step reconstruction loss during training.

Table 2: Optimal reconstruction loss of the models

Model	Iteration	50-step loss	2,000-step loss
vanilla	30,500	0.014509	0.006171
BN	30,500	0.017199	0.006355
WN	463,000	0.013010	0.005524

for evaluation in case it converges with a much worse 50-step reconstruction loss than at its optimal iteration. We consider that training has converged if both the 50-step reconstruction loss and the generated samples stay stable for long enough.

We observed mode collapse in the vanilla and BN models. To reduce the possibility that these observations are due to random factors, we repeated the training procedure of these two models for 3 times. The result from the best training instance is presented here. Additional training instances of vanilla and BN models can be found in appendix C.1.

The same set of experiments were also conducted on LSUN bedroom and CIFAR-10 datasets, see appendices C.3 and C.4.

5.2 Reconstruction

The (per-pixel) 50-step reconstruction loss of the three models is shown in figure 1 for the first 150,000 iterations. The vanilla and BN model were considered to have collapsed. The WN model was trained to 700,000 iterations and converged to a near-optimal state (see appendix B) so no “final” model was evaluated.

The lowest 50-step loss recorded during training, the iteration at which this minimum loss is achieved, and loss of 2,000-step evaluation for each model is listed in table 2. WN achieves about 10.5% lower 2,000-step reconstruction loss than the vanilla model, while for BN the loss is 3% higher. We can also see from the loss curve that until the vanilla model collapses, BN never achieved a better reconstruction loss.

While the WN model achieved best overall reconstruction loss, it started out a bit worse than the vanilla model and took until iteration 135,000 to surpass the best vanilla model. We had a simple trick that further speeds up the decrease of reconstruction loss of the WN model, presented in appendix C.2

We also visually inspected the reconstruction results. Selected reconstructed samples are compared to the original test samples in figure 2. These samples are selected such that all three models give reasonable results. Additional random samples can be found in appendix B. The WN model captures details (e.g. facial expression, texture of hair, subtle color variation) much more accurately. Samples reconstructed by the BN model look more blurry and have more artifacts.



Figure 2: Selected 2,000-step reconstruction results. From left to right in each group: test sample, vanilla reconstruction, BN reconstruction, WN reconstruction.

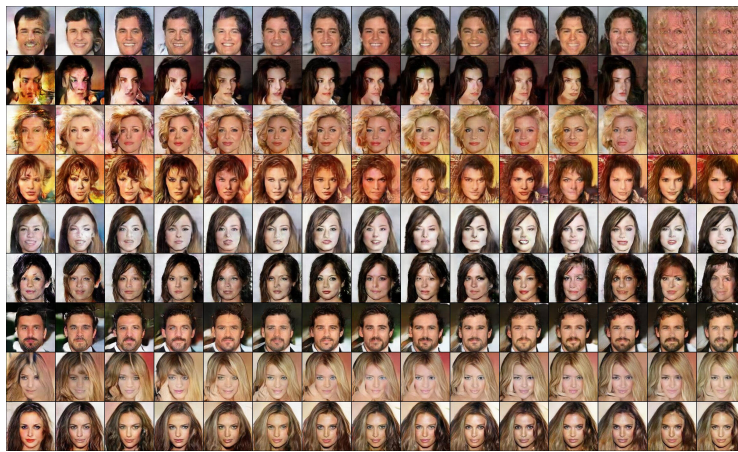


Figure 3: Evolution of samples during training. Top 3 rows: vanilla; Middle 3 rows: BN; Bottom 3 rows: WN. Columns: every 10,000 iterations from 10,000 to 150,000.

5.3 Stability

As can be seen from figure 1, after achieving their optimal reconstruction loss relatively early during their training, the reconstruction of vanilla and BN models started to get worse. For the vanilla model, the loss went up slowly, then in a relatively short time around iteration 135,000, the generator collapses to generating the same output and the reconstruction loss went up suddenly. For the BN model, at around 40,000 iterations, the loss started to show excessive fluctuation.

While not shown here, the WN model kept improving steadily until 300,000 iterations and then remained largely stable.

We can also visualize this (in)stability by checking samples generated from the same code at different iterations, as shown in figure 3. The WN model is visibly more stable as sample generated from the same code remain mostly constant across a time scale of 100,000 iterations, and the generated samples are slowly improving, while the other two models produce more random variations. Additional visual analysis can be found in appendix B along with more samples.

We consider the stability of our weight-normalized model to be comparable to Wasserstein GAN [1]. We include a discussion of the connections in appendix D. Importantly, this improvement in stability is achieved solely by changing the parametrization of the network, rather than engineering new loss functions (e.g. in BEGAN [3]), training objectives (e.g. in improved WGAN [7]) or network structures (e.g. in EBGAN [15]).

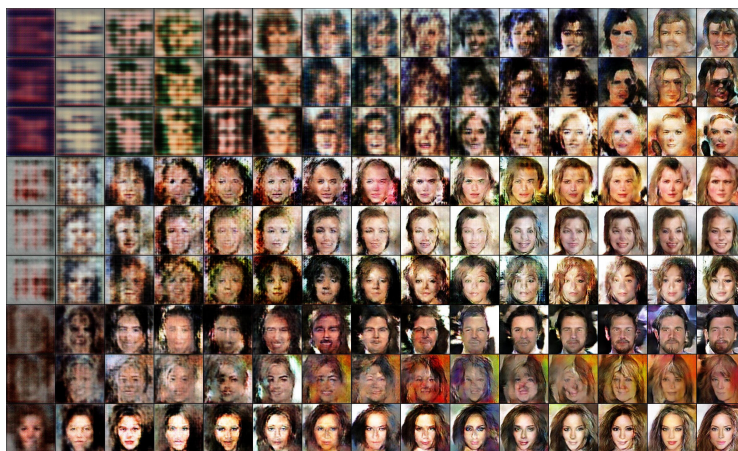


Figure 4: Evolution of samples during early stage of training. Top 3 rows: vanilla; Middle 3 rows: BN; Bottom 3 rows: WN. Columns are samples from iterations 100, 200, 300, 400, 500, 600, 800, 1000, 1200, 1500, 2000, 2500, 3000, 4000 and 5000.

5.4 Training speed

We compare the training speed of the three models by checking their generated samples during early stage of training, as shown in figure 4. It is evident that Batch Normalization does have the claimed effect of accelerate training, and the effect of Weight Normalization is comparable. Note that the WN model is already getting a idea about human faces at as early as iteration 100.

But we argue that this accelerated training is not very useful beyond serving as a fast sanity check of the network, as it only affects the earliest stage of training. As can be seen in figure 3, at iteration 10,000, the visual quality of samples generated by the three models are comparable, and no one is making a noticeably faster progress than the other. In addition, being able to generate visually plausible samples earlier does not translate into faster improvement of reconstruction.

We also point out that BN permits a higher learning rate: training of the vanilla and WN models start to fail often with a learning rate of 0.0002, while the BN model is still trainable with a learning rate of 0.001. However, we found that a increased learning rate did not make the BN model train faster. Instead, it further harms the stability of the model.

6 Conclusion

We proposed an alternative formulation of Weight Normalization, which provides an augmentation to the method in [12] and fixes an error in [2].

We also proposed using the mean Euclidean distance between test samples and closest generated samples found by performing gradient descent on latent code as a way of evaluating Generative Adversarial Networks.

We trained DCGAN [11] variants with different normalization methods for image generation on several image sets of different scale. Contrary to common belief, batch-normalized models is found to perform worse in reconstructing test samples and expose higher instability during training, in terms of both reconstruction error and visual quality of generated samples.

Instead, our version of weight normalization does actually improve reconstruction error and training stability considerably. In conclusion, Batch Normalization should not be used in Generative Adversarial Networks. Weight Normalization should be used instead.

References

- [1] Martin Arjovsky, Soumith Chintala, and Léon Bottou. Wasserstein gan. *arXiv preprint arXiv:1701.07875*, 2017.

- [2] Devansh Arpit, Yingbo Zhou, Bhargava U Kota, and Venu Govindaraju. Normalization propagation: A parametric technique for removing internal covariate shift in deep networks. *arXiv preprint arXiv:1603.01431*, 2016.
- [3] David Berthelot, Tom Schumm, and Luke Metz. Began: Boundary equilibrium generative adversarial networks. *arXiv preprint arXiv:1703.10717*, 2017.
- [4] Soumith Chintala, Emily Denton, Martin Arjovsky, and Michael Mathieu. How to train a gan? tips and tricks to make gans work. <https://github.com/soumith/ganhacks>, 2016. Accessed: 2017-02-26.
- [5] Emily L Denton, Soumith Chintala, Rob Fergus, et al. Deep generative image models using a laplacian pyramid of adversarial networks. In *Advances in neural information processing systems*, pages 1486–1494, 2015.
- [6] Ian Goodfellow, Jean Pouget-Abadie, Mehdi Mirza, Bing Xu, David Warde-Farley, Sherjil Ozair, Aaron Courville, and Yoshua Bengio. Generative adversarial nets. In *Advances in neural information processing systems*, pages 2672–2680, 2014.
- [7] Ishaan Gulrajani, Faruk Ahmed, Martin Arjovsky, Vincent Dumoulin, and Aaron Courville. Improved training of wasserstein gans. *arXiv preprint arXiv:1704.00028*, 2017.
- [8] Sergey Ioffe and Christian Szegedy. Batch normalization: Accelerating deep network training by reducing internal covariate shift. *arXiv preprint arXiv:1502.03167*, 2015.
- [9] Diederik P Kingma and Max Welling. Auto-encoding variational bayes. *arXiv preprint arXiv:1312.6114*, 2013.
- [10] Ziwei Liu, Ping Luo, Xiaogang Wang, and Xiaoou Tang. Deep learning face attributes in the wild. In *Proceedings of International Conference on Computer Vision (ICCV)*, December 2015.
- [11] Alec Radford, Luke Metz, and Soumith Chintala. Unsupervised representation learning with deep convolutional generative adversarial networks. *arXiv preprint arXiv:1511.06434*, 2015.
- [12] Tim Salimans and Diederik P Kingma. Weight normalization: A simple reparameterization to accelerate training of deep neural networks. In *Advances in Neural Information Processing Systems*, pages 901–901, 2016.
- [13] Lucas Theis, Aäron van den Oord, and Matthias Bethge. A note on the evaluation of generative models. *arXiv preprint arXiv:1511.01844*, 2015.
- [14] Tijmen Tieleman and Geoffrey Hinton. Lecture 6.5-rmsprop: Divide the gradient by a running average of its recent magnitude. *COURSERA: Neural networks for machine learning*, 4(2), 2012.
- [15] Junbo Zhao, Michael Mathieu, and Yann LeCun. Energy-based generative adversarial network. *arXiv preprint arXiv:1609.03126*, 2016.

A Proof of equivalence between non-normalized network and strict weight-normalized network with one affine weight-normalized layer at the end

Consider two networks with $(2n + 1)$ layers each. The first network is a non-normalized network, where layers $(2k + 1)$ ($0 \leq k \leq n$) are linear layers and layers $2k$ ($1 \leq k \leq n$) are ReLU layers. The second network is a weight-normalized network, where layers $(2k + 1)$ ($0 \leq k \leq n - 1$) are strict weight-normalized layers, layer $(2n + 1)$ is an affine weight-normalized layer, and layers $2k$ ($1 \leq k \leq n$) are translated ReLU layers.

We make the following claim:

Claim 1. *The aforementioned two networks are capable of representing the same set of functions.*

First, we proof that a linear-and-ReLU combination is equivalent to a strict-weight-normalized-and-TReLU combination, if both are augmented by a learned affine transformation at the end.

Lemma 2. *A linear layer, followed by a ReLU layer, followed by an affine transformation, is equivalent to a strict weight-normalized layer, followed by a TReLU layer, followed by an affine transformation.*

Proof. For simplicity we consider the case where the first layer has only one output neuron. Then, a linear layer, followed by a ReLU layer, followed by an affine transformation, would be

$$y = \text{ReLU}(\mathbf{w}^T \mathbf{x} + \alpha) \cdot \gamma + \beta$$

while a strict weight-normalized layer, followed by a TReLU layer, followed by an affine transformation, would be

$$y = \text{TReLU}_{\alpha'}\left(\frac{\mathbf{w}'^T \mathbf{x}}{\|\mathbf{w}'\|}\right) \cdot \gamma' + \beta'$$

where $\mathbf{w}, \mathbf{w}', \alpha, \alpha', \beta, \beta', \gamma$ and γ' are all learned parameters. The transformation

$$\begin{cases} \mathbf{w}' &= \mathbf{w} \\ \alpha' &= -\frac{\alpha}{\|\mathbf{w}\|} \\ \beta' &= \beta + \alpha \cdot \gamma \\ \gamma' &= \|\mathbf{w}\| \cdot \gamma \end{cases} \quad \text{and} \quad \begin{cases} \mathbf{w} &= \mathbf{w}' \\ \alpha &= -\|\mathbf{w}'\| \cdot \alpha' \\ \beta &= \beta' + \alpha' \cdot \gamma' \\ \gamma &= \frac{\gamma'}{\|\mathbf{w}'\|} \end{cases}$$

establishes a one-to-one correspondence between these two forms. □

Then, we have these observations:

Lemma 3. *A linear preceded by an affine transformation is equivalent to a single linear layer.*

Lemma 4. *A linear layer is equivalent to an affine weight-normalized layer.*

The proofs are trivial.

Now we demonstrate the proof of claim 1 by transforming network 1 to network 2:

We do the following one by one for each k from 1 to $(n - 1)$: first, we add an affine transformation between ReLU layer $2k$ and linear layer $(2k + 1)$. Then, we exchange linear layer $(2k - 1)$ and ReLU layer $2k$ for a strict weight-normalized layer and a TReLU layer. Then, we remove the additional linear transformation. The addition and removal of affine transformation does not change the expressiveness of the network since a linear layer succeeds it. With an affine layer in place, the exchange does not change the expressiveness of the network either.

Finally, we change the last linear, layer $(2n + 1)$, to an affine weight-normalized layer.



Figure 5: Samples generated by vanilla model, every 100 iterations from 134,000 to 135,400

B Additional samples and analysis

Here we show more generated samples from the three models. In addition, some problem with GAN training can only be detected by visually inspecting a large amount of samples. Due to space limitations we were not able to discuss them in section 5, so we present them here.

B.1 Vanilla model

Figure 6 shows samples generated by vanilla model from the same set of random codes, at iteration 30,500 (optimal iteration) and 120,000. Samples generated at 120,000 iterations actually have better visual quality on average if we look at each sample individually. But notice how the diversity of the samples has decreased: the lower half of the figure is dominated by yellow and brown colors and are darker than the upper half. Even more subtle, the lower half has less variation in facial expressions. Even the diversity of gender is decreasing: some clear male faces in the upper half becomes more feminine in the lower half.

During the training process, past a certain point, samples start to evolve towards the same direction: while samples remain different, in each iteration they make very similar changes. In this process, difference between samples is gradually lost. This corresponds to the slow and steady increase of the reconstruction loss. At around 130,000 iterations, this process suddenly accelerates and finally at some point, the model collapses, as shown in figure 5.

Interestingly, this seems like the reverse of the early stage: the training usually starts with each code generating similar output and making nearly the same changes until the generated samples start to gain diversity.

B.2 Batch-normalized model

Figure 7 shows samples generated by BN model from the same set of random codes, at iteration 30,500 (optimal iteration) and 110,000. At a first glance, it does not show the decrease in diversity as the vanilla model. But after comparing the samples carefully, we can discover certain repeatedly-occurring features. To see this more clearly, in figure 8 we picked and rearranged several samples from figure 7.

We identified two groups from samples generated at iteration 110,000. Within each group, while the appearance of the face vary considerably, they are making almost the exact same expression. When comparing these samples from samples generated from the same codes at iteration 30,500, we found that the second group is newly formed while the first such group has already long existed, indicating that the BN model had limited diversity even at its optimal iteration.

This shows a different route towards mode collapse: as the training progresses, some features become dominant. Several such features may occur. While the samples may otherwise retain their difference, more and more samples start to acquire these dominating features. In the extreme case, only a handful of different possible output remain at the end.



Figure 6: Random samples generated by vanilla model. Upper half: iteration 30,500. Lower half: Iteration 120,000.

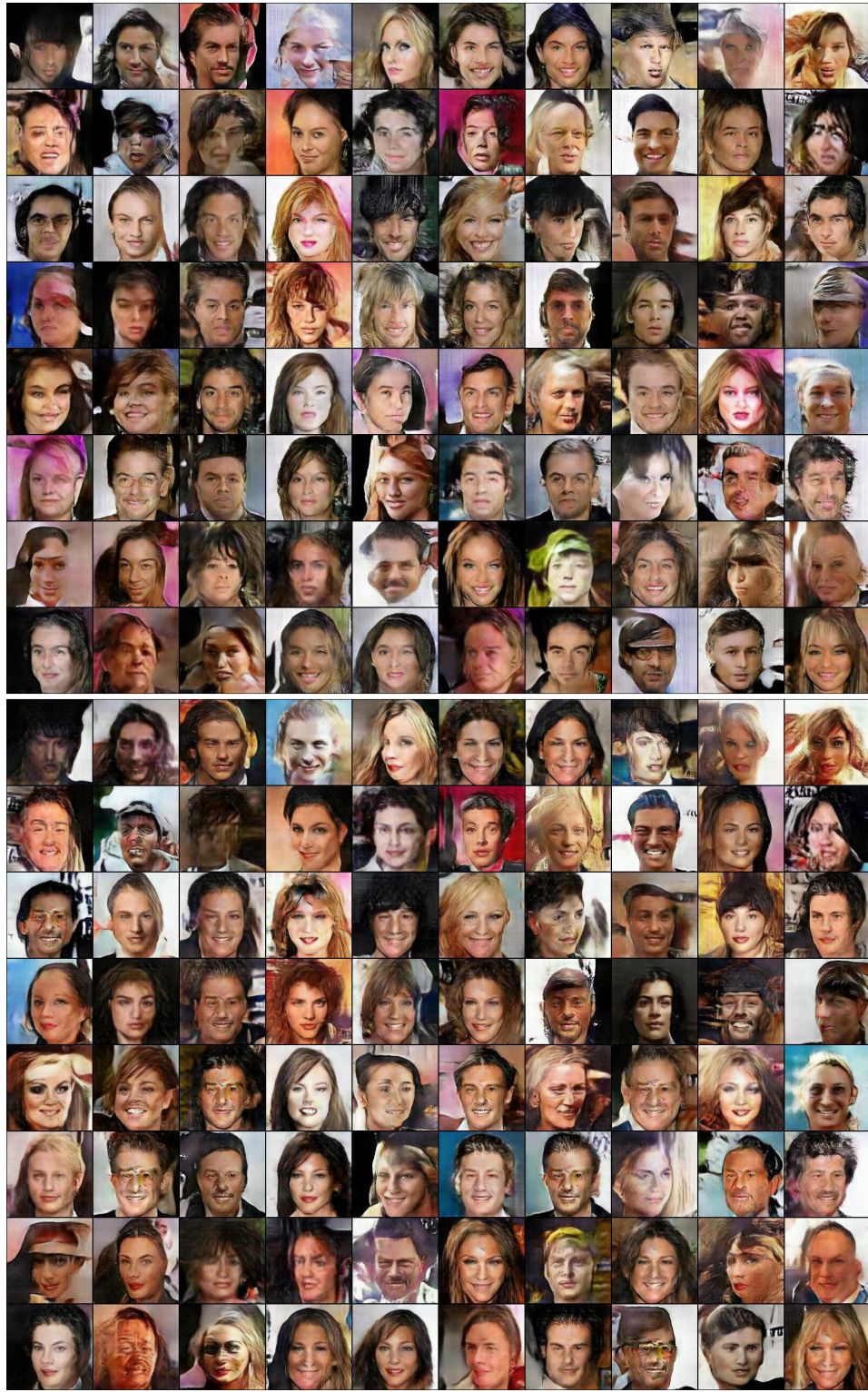


Figure 7: Random samples generated by BN model. Upper half: iteration 30,500. Lower half: Iteration 110,000.



Figure 8: Selected samples from figure 7. Row 1 and 3 are from iteration 30,500. Row 2 and 4 are corresponding samples from iteration 110,000.



Figure 9: Samples generated by BN model instance 3, every 100 iterations from 38,300 to 39,200

Alternatively, mode collapse may suddenly happen, as is the case for the “failed” training instance 3 in appendix C.1. We show the samples generated when the model collapses in figure 9. There was no clear sign of decreased diversity prior to the sudden collapse.

B.3 Weight-normalized model

Figure 10 shows random samples generated by the optimal WN model. Diversity-wise it is not ideal as the samples still display a lack of color variation and a unbalanced gender ratio comparing to the true distribution, but they show more variation than the vanilla model and less subtle recurring features comparing to the BN model. The individual samples are of higher quality on average as well. Also note the relative low rate of “failed” or highly implausible samples.

Figure 11 shows the 50-step reconstruction loss recorded during the whole training process of the WN model. The loss remain almost constant after iteration 300,000, which demonstrates the stability of the WN model.

B.4 Random reconstructed samples

Figure 12 shows a random selection of reconstructed samples.



Figure 10: Random samples generated by WN model at iteration 463,000

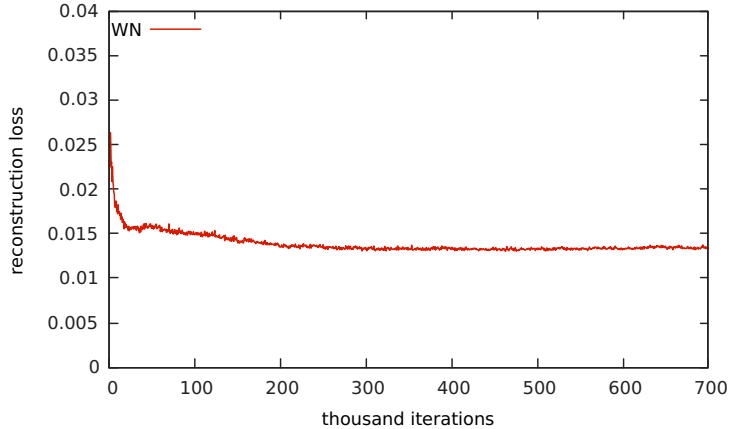


Figure 11: 50-step reconstruction loss during training of WN model

Table 3: Optimal reconstruction loss of repeated training of vanilla model.

Instance	Iteration	50-step loss
vanilla-1	30,500	0.014509
vanilla-2	34,500	0.014703
vanilla-3	31,000	0.014734

C Additional experiments

C.1 Additional training instances of vanilla and BN models

Figures 13 and 14 and tables 3 and 4 shows the reconstruction loss recorded during all training instances of the vanilla and batch-normalized models.

We can see that the three instances of vanilla model gave almost identical loss curves, achieved similar optimal loss at similar times, and mode collapse happened around the same time.

In contrast, in addition to instability observed in each individual training instance, the batch-normalized also showed “meta-instability” as the behavior differed considerably between each training instance. Notably, in the third instance, mode collapse happened very soon. The training did recover to some extent, but the model was never able to regain the same sample diversity as before the mode collapse.

C.2 Additional models

First, we introduce our extra trick. Clipping the bias term α of the first two TPreLU layers in the generator to the range $[0, 1]$ is found to help with training. This trick was discovered by accident and there is no justification for its use.

For completeness, we also compare different formulations of Weight Normalization. The first one is a full-affine WN model, constructed from the WN model by replacing all strict weight-normalized layers by affine weight-normalized layers and all TPreLU layers by PReLU layers. The second one is a model with Weight Normalization plus mean-only Batch Normalization, as used in [12],

Table 4: Optimal reconstruction loss of repeated training of batch-normalized model.

Instance	Iteration	50-step loss
BN-1	37,000	0.017349
BN-2	30,500	0.017199
BN-3	16,000	0.018810



Figure 12: Random reconstructed test samples. From left to right in each group: test sample, vanilla reconstruction, BN reconstruction, WN reconstruction.

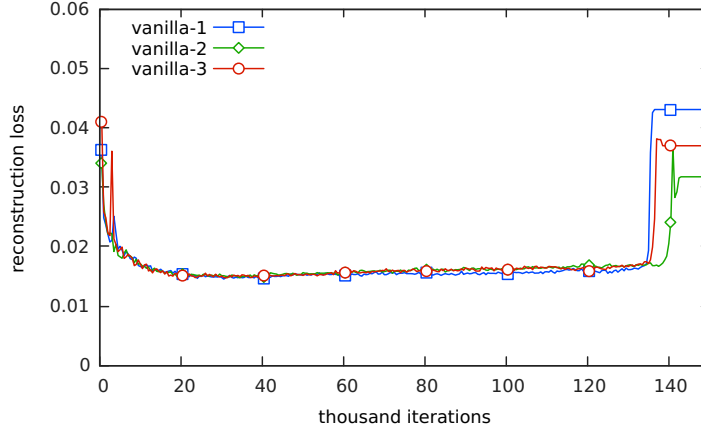


Figure 13: 50-step reconstruction loss of repeated training of vanilla model.

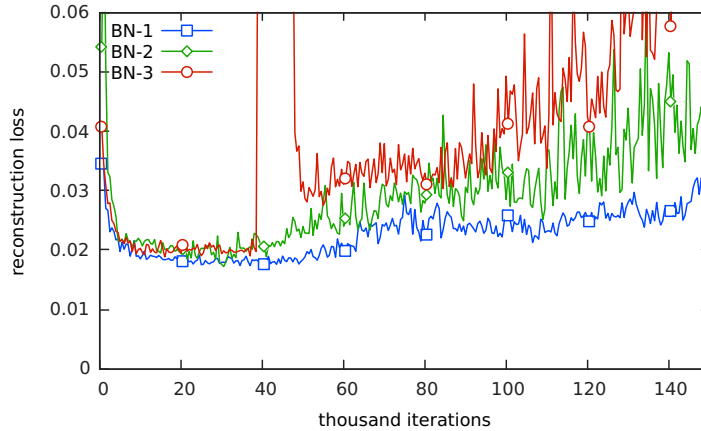


Figure 14: 50-step reconstruction loss of repeated training of batch-normalized model.

constructed by taking the affine WN model and add mean-only Batch Normalization at places where normal Batch Normalization layers would be used in the BN model.

The reconstruction loss for the first 150,000 steps are shown in figure 15 and table 5. Result of WN model included for comparison.

Although less severe than the BN model, WN with mean-only BN shows the characteristic fluctuation of the BN model, and is also worse than the vanilla model. We consider the major advantage of WN over BN to be its being independent from batch statistics. With the addition of mean-only BN, this dependency is introduced back, which harms the stability of the model.

The WN model with weight clipping is found to further speed up training during the early stage. It harms the expressiveness of the network, though. But we can always simply remove weight clipping and revert to a normal WN model when desirable.

Table 5: Optimal reconstruction loss of additional models.

Model	Optimal iteration	50-step loss
affine-WN	51,000	0.014034
WN+mean-BN	19,500	0.016639
WN+clipping	129,000	0.013201
WN	463,000	0.013010

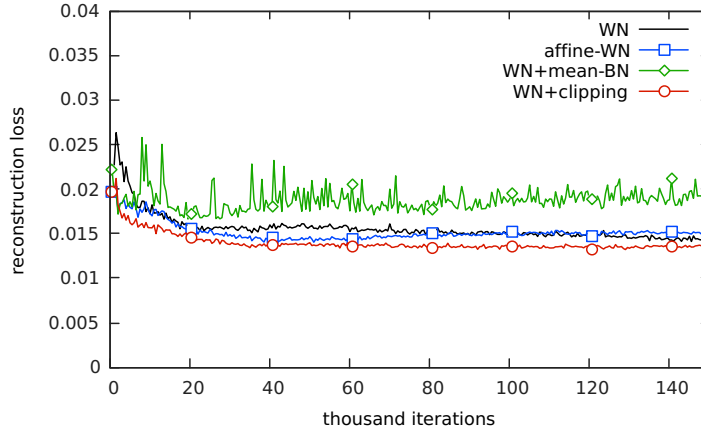


Figure 15: 50-step reconstruction loss during training of additional models.

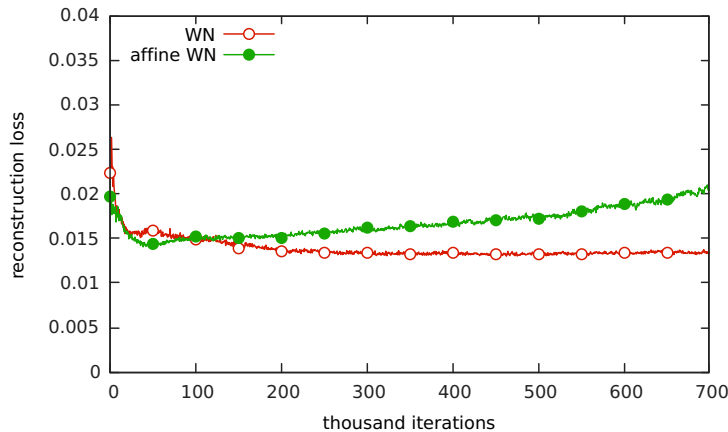


Figure 16: 50-step reconstruction loss during training of the WN and affine-WN models

We are particularly interested in the comparison between the WN model and the affine-WN model, as it tests our formulation of Weight Normalization against the one originally proposed in [12]. For this purpose, we trained the affine-WN model to iteration 700,000 as well. Figure 16 shows the comparison of their reconstruction loss during training.

After making a quick descent at the beginning, the 50-step reconstruction loss of the affine-WN model started to increase steadily. Unlike the vanilla model however, the generated samples kept stable and high-quality, so we took both the optimal model and the model at iteration 700,000 for evaluation. The results are compared with the WN model in table 6.

Surprisingly the affine-WN model at iteration 700,000 gives equally good 2,000-step reconstruction as iteration 51,000 when the best 50-step reconstruction is achieved, although its 50-step reconstruction is much worse. Both of them, however, are about 7.5% worse than the WN model.

Table 6: Optimal and converged reconstruction loss of WN and affine-WN models

Model	Iteration	50-step loss	2,000-step loss
affine-WN	51,000	0.014034	0.005941
affine-WN	700,000	0.020478	0.005939
WN	463,000	0.013010	0.005525

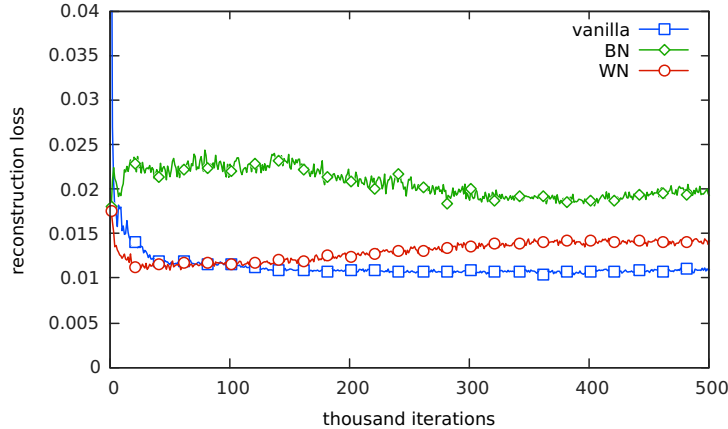


Figure 17: Reconstruction loss during training on CIFAR-10.

The difference between the two models tells us something interesting: the WN model is equivalent to the affine-WN model in terms of the set of functions they can express, but has fewer parameters as the learned affine transformations are removed except for the last layer. By removing these redundant parameters, we made both a quantitative improvement and a qualitative difference, as the more complex model degrades while the simpler model does not. Thus, we suggest that our version of Weight Normalization be experimented on other tasks to see if it can improve on the original formulation as well.

C.3 Experiments on CIFAR-10 dataset

There are 60,000 images (training plus validation) of size 32×32 in the CIFAR-10 dataset. We construct models in similar ways as for CelebA but start from 96 output channels for the first convolution layer and stop down-convolution when the spatial size of the feature map is 4×4 . The length of the code (256) and training batch size (32) remains the same.

We use 58,000 images for training and 2,000 images for evaluation. During training, evaluation is performed every 1,000 training iterations on 400 images, with 50 gradient descent steps. Final evaluation is performed on whole test set with 2,000 gradient descent steps.

BN is still the worst model but the vanilla and WN models have seemingly changed roles: now the WN model achieves optimal loss early and starts to get worse but the vanilla model kept improving. However, both models converge, as shown by the flat section in the loss curve, between iterations 400,000 and 500,000. So we take these two models at iteration 500,000 for evaluation in addition to the optimal 50-step models. The BN model does not actually converge, as the “recurring feature” discussed in section B occurred and the feature changes rapidly. For completeness however, we also take the BN model from iteration 500,000 for evaluation.

The seemingly worse 500,000-iteration WN model turned out to give the best 2,000-step reconstruction result, which is unexpected. A more careful examination of the reconstruction process revealed that the 500,000-iteration WN model achieved better reconstruction than the optimal vanilla model at around 400th reconstruction step. We acknowledge that this exposes a weakness of our evaluation method: performing the reconstruction for too few steps may give inaccurate results, while too many steps would be time-consuming and make it unsuitable for monitoring training process.

Figure 18 shows random samples generated by the three models, at their optimal iteration and at iteration 500,000. While the visual quality of samples from all models are good, diversity wise, the results are consistent with the analysis in appendix B: the vanilla samples look dull and dominated by one color (green); the BN samples show a recurring feature (marked with red border).

Figure 19 shows random test samples and reconstructed samples.



Figure 18: CIFAR-10 samples. Top to bottom: vanilla model, BN model, WN model. Left: optimal iteration. Right: iteration 500,000.

Table 7: Optimal and converged reconstruction loss of the models on CIFAR-10

Model	Iteration	50-step loss	2,000-step loss
vanilla	387,000	0.010382	0.003413
BN	1,000	0.017987	0.004904
WN	50,000	0.010906	0.003509
vanilla	500,000	0.010948	0.003414
BN	500,000	0.019287	0.005421
WN	500,000	0.014195	0.003269

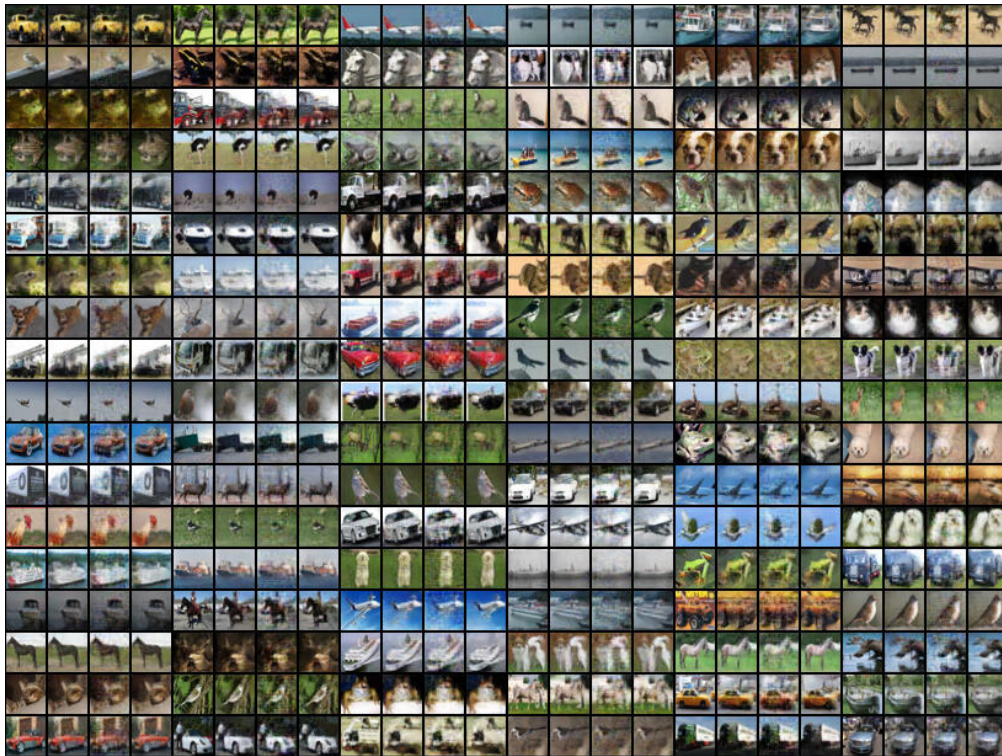


Figure 19: CIFAR-10 reconstructions. Each group, left to right: test sample, vanilla model, BN model, WN model.

C.4 Experiments on LSUN bedroom dataset

There are 3,033,042 images in the bedroom class of the LSUN dataset, with images having 256 pixels on the shorter side. Unlike many published results on this dataset, we use the full-sized images: we crop to the center 256×256 patch but does not down-sample the image. We construct models in similar ways as for CelebA, but stop down-convolution when the spatial size of the feature map is 4×4 and use a code length of 512. Due to the large size of the images and the network, we reduce the batch size to 12 to save time and memory.

We use 2,000 images for evaluation and the rest for training. During training, evaluation is performed every 1,000 training iterations on 200 images, with 50 gradient descent steps. Final evaluation is performed on whole test set with 2,000 gradient descent steps.

For the vanilla model, training fails constantly, even when we reduce the learning rate by a factor of 10 (to 10^{-5}), so only the BN and WN models are compared here. The two models are trained to iteration 300,000. The reconstruction loss is shown in figure 20 and table 8.

Random samples generated by the two models are shown in figures 21 and 22. Reconstruction of random samples are shown in figure 23.

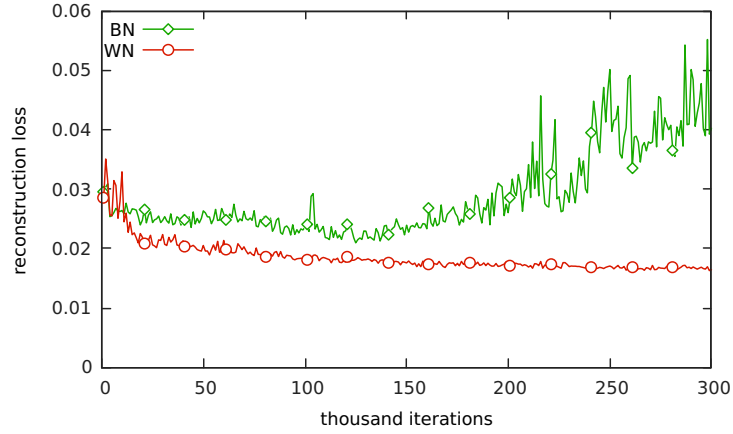


Figure 20: Reconstruction loss during training on LSUN bedroom dataset.

Table 8: Reconstruction loss of the models on LSUN bedroom dataset

Model	Optimal iteration	50-step loss	2,000-step loss
BN	125,000	0.020943	0.011051
WN	299,000	0.016266	0.009180

In the BN samples, recurring tile-like artifacts are observed. The best quality samples generated by the BN model look sharp and clean, while the WN model got details more accurately.

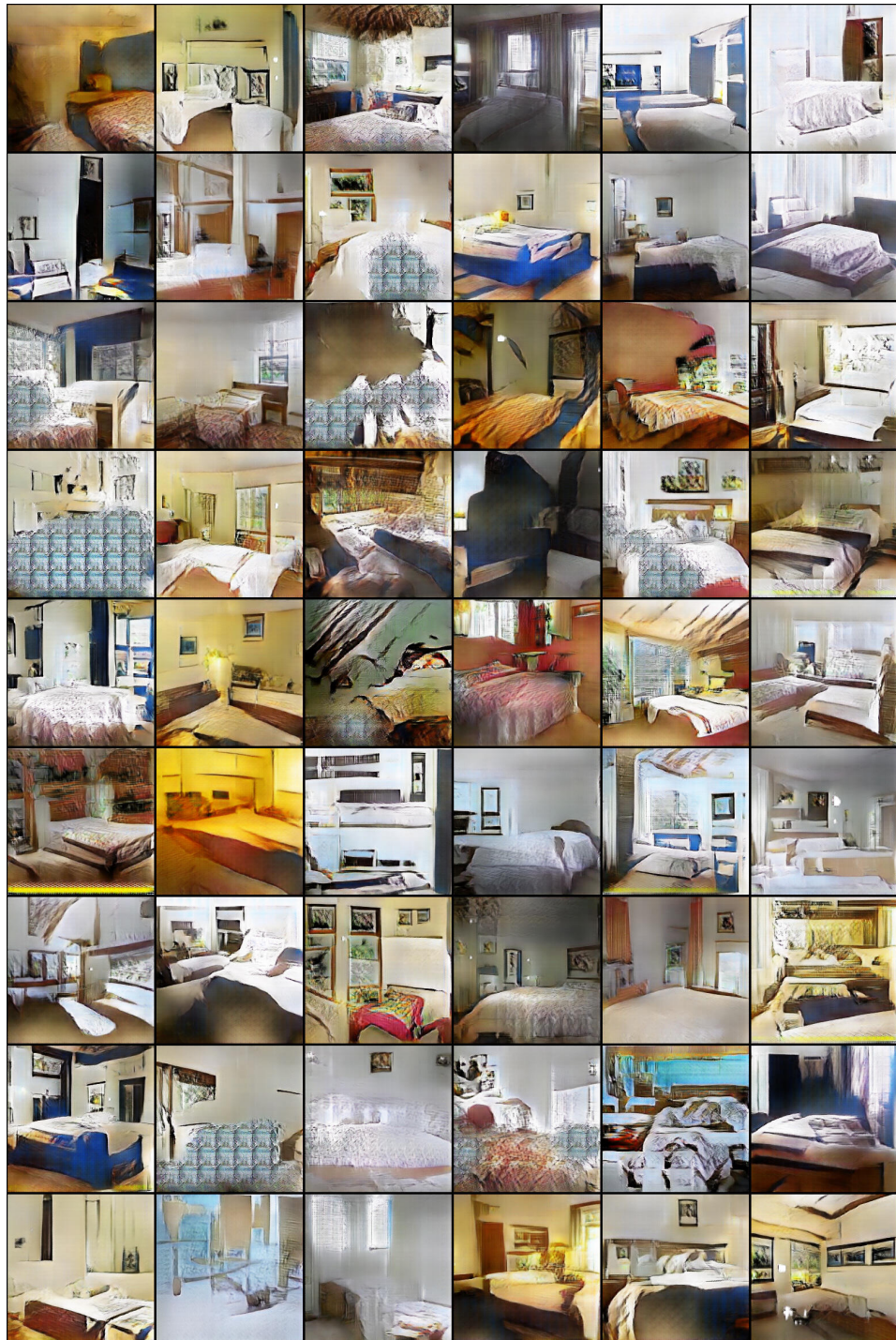


Figure 21: LSUN samples generated by the BN model at iteration 125,000

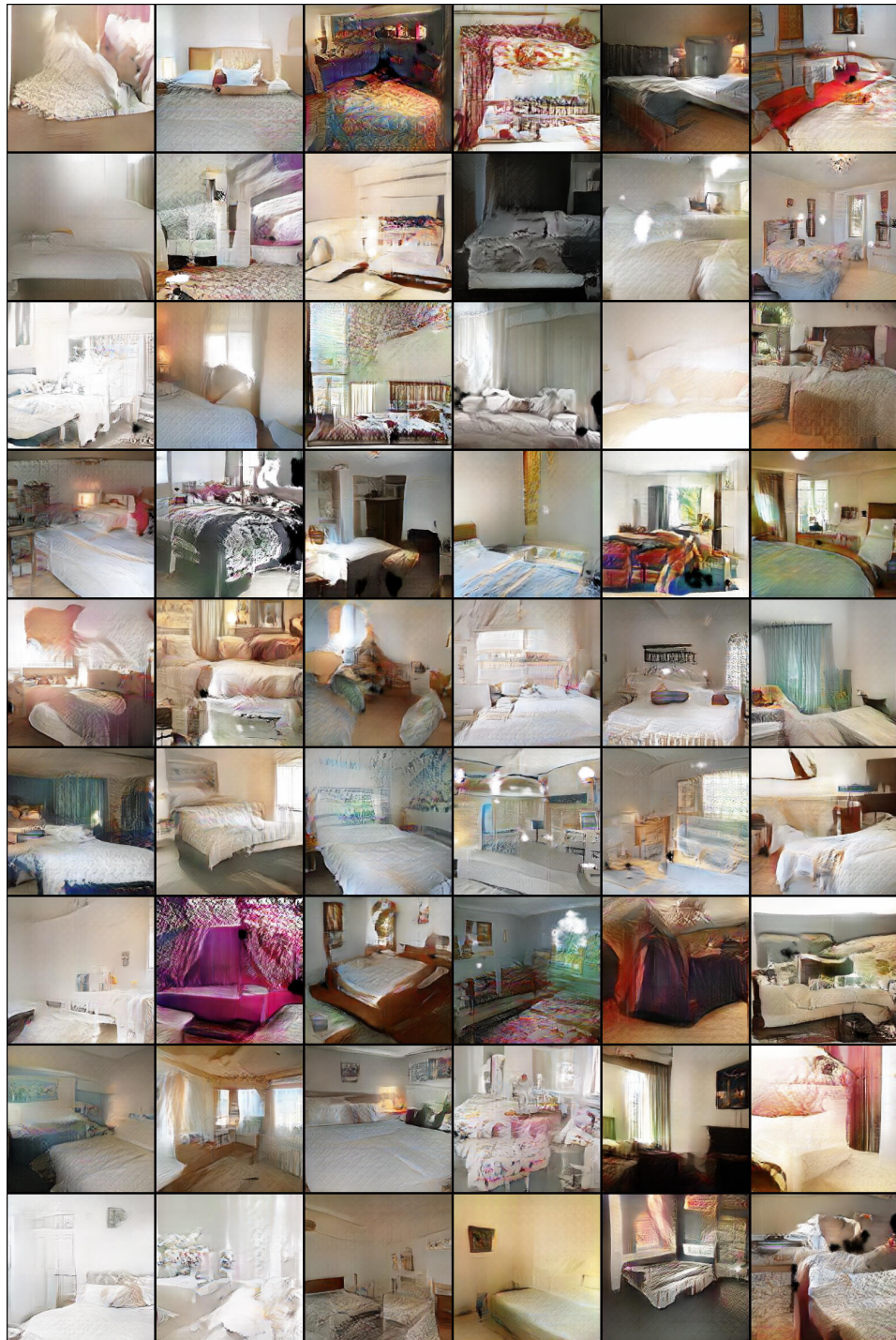


Figure 22: LSUN samples generated by the WN model at iteration 299,000

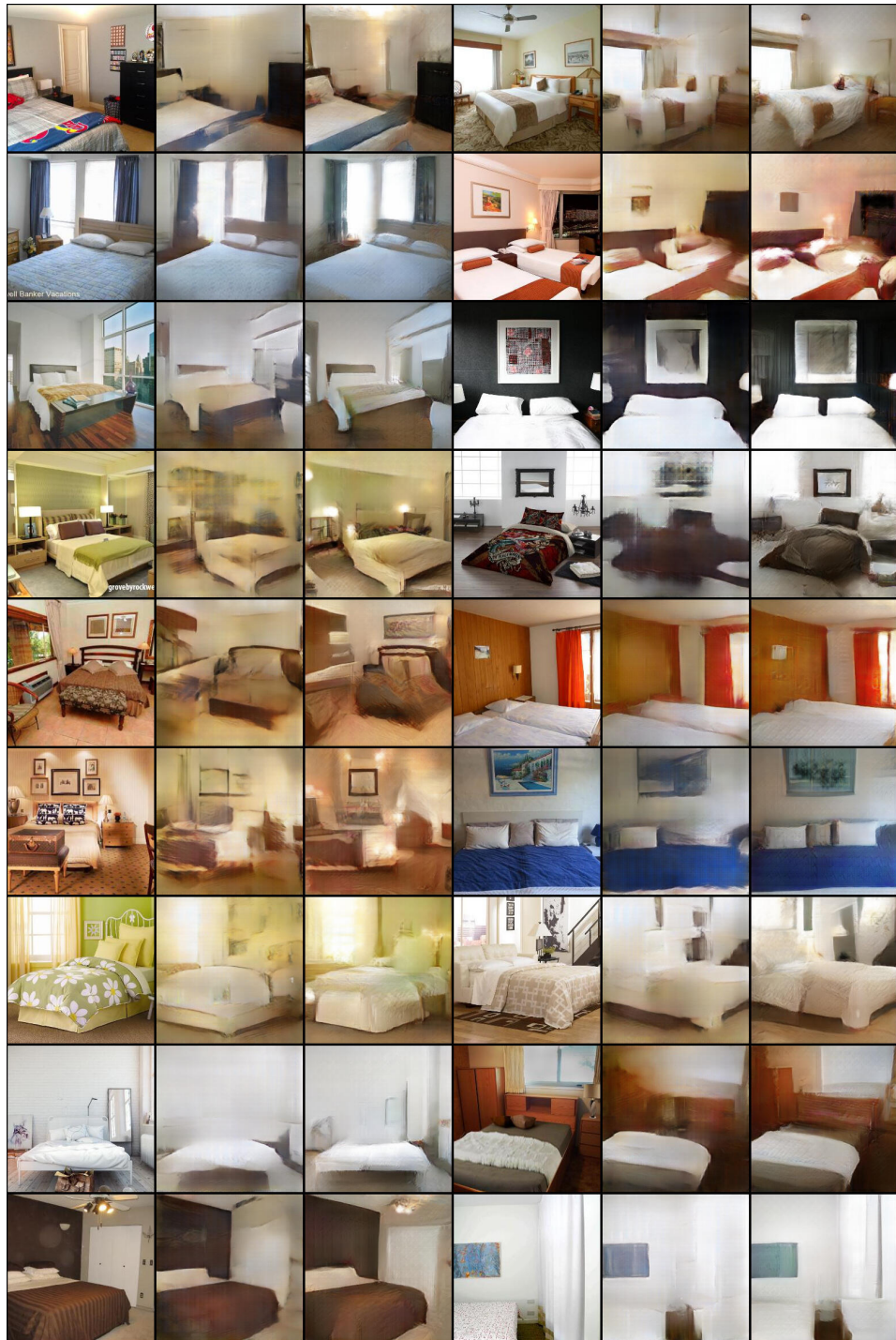


Figure 23: LSUN reconstructions. Each group, left to right: test sample, BN model, WN model.

D Connection to Wasserstein GAN

In Wasserstein GAN [1], the discriminator is replaced with a critic that is K -Lipschitz-continuous for some constant K that depends only on the structure of the network. To achieve this, they clipped the parameters of the critic network to a small window $[-0.01, 0.01]$ after each parameter update during training.

We claim that our weight-normalized discriminator is Lipschitz-continuous with a small modification:

Claim 1. *The weight-normalized discriminator proposed in this paper is K -Lipschitz-continuous for some constant K if the sigmoid layer is removed and the only affine weight-normalized layer is replaced by a strict weight-normalized layer.*

To see this, we first prove the following lemma:

Lemma 2. *For a strict weight-normalized layer*

$$y_i = \frac{\mathbf{w}_i^T \mathbf{x}}{\|\mathbf{w}_i\|}$$

where $\mathbf{x} \in \mathbb{R}^n$, $\mathbf{y} \in \mathbb{R}^m$, $\mathbf{W} \in \mathbb{R}^{n \times m}$ is the weight matrix and \mathbf{w}_i is the i -th column of \mathbf{W} , if the loss function of the network is L , then

$$\sum_{i=1}^n \left| \frac{\partial L}{\partial x_i} \right| \leq \sqrt{n} \cdot \sum_{i=1}^m \left| \frac{\partial L}{\partial y_i} \right| \quad (8)$$

Proof.

$$\begin{aligned} \sum_{i=1}^n \left| \frac{\partial L}{\partial x_i} \right| &= \sum_{i=1}^n \sum_{j=1}^m \left(\left| \frac{\partial y_j}{\partial x_i} \right| \cdot \left| \frac{\partial L}{\partial y_j} \right| \right) \\ &= \sum_{j=1}^m \left(\left| \frac{\partial L}{\partial y_j} \right| \sum_{i=1}^n \left| \frac{\partial y_j}{\partial x_i} \right| \right) \\ &= \sum_{j=1}^m \left(\left| \frac{\partial L}{\partial y_j} \right| \sum_{i=1}^n \frac{|w_{ij}|}{\|\mathbf{w}_j\|} \right) \\ &\leq \sum_{j=1}^m \left(\left| \frac{\partial L}{\partial y_j} \right| \cdot \sqrt{n} \right) \\ &= \sqrt{n} \cdot \sum_{j=1}^m \left| \frac{\partial L}{\partial y_j} \right| \end{aligned}$$

□

For a strict weight-normalized convolution layer with c_I input channels and kernel size $k_W \times k_H$, change \sqrt{n} in inequality 8 to $\sqrt{c_I \cdot k_W \cdot k_H}$.

Note that in our implementation, the learned slope of parametric ReLU layers are clipped to $[0, 1]$, so the following is obvious:

Lemma 3. *For a TPreLU layer with input \mathbf{x} and output \mathbf{y} in \mathbb{R}^n ,*

$$\sum_{i=1}^n \left| \frac{\partial L}{\partial x_i} \right| \leq \sum_{i=1}^n \left| \frac{\partial L}{\partial y_i} \right|$$

Now it is easy to see that claim 1 is true since for each layer the sum of absolute value of gradients grows by at most a constant factor. So with such a modification, our discriminator changes into a WGAN critic.